UV−Visible Absorption Spectroscopy To Examine Shock-Induced Decomposition in Neat Nitromethane

J. M. Winey and Y. M. Gupta*

Shock Dynamics Center and Department of Physics, Washington State University, Pullman, Washington 99164-2814

Received: June 4, 1997; In Final Form: August 25, 1997[⊗]

Time-resolved UV−visible absorption spectroscopy was used to examine chemical decomposition in neat liquid nitromethane (NM) subjected to stepwise shock loading to 19 GPa. Up to a peak pressure (temperature) of 13.8 GPa (854 K), no sign of chemical reaction was observed in the nπ* absorption band centered at 270 nm. For shock compression resulting in peak temperatures above 940 K, extensive reaction was indicated by irreversible red-shifting of the absorption band edge that occurred after peak pressure was reached. This red-shift was followed by a loss of transmission through the sample, which was attributed to the formation of absorbing reaction products. Comparison of these reaction-induced spectral changes with previous absorption results for NM sensitized by ethylenediamine (EDA) suggests that the presence of the amine causes a change in the early stages of shock-induced decomposition. An induction time was observed between the attainment of peak pressure and the onset of reaction-induced spectral changes in neat NM. Significant decreases in the induction time were produced by modest increases of 25−50 K in the initial sample temperature. The induction time data are consistent with the thermal explosion model of shock initiation in energetic materials. The observed induction time correlates well with the final shock temperature; no pressure dependence is observable within the pressure range examined here. Measured induction times for the absorption experiments are consistently shorter than for continuum experiments reaching similar temperatures likely because the absorption technique probes earlier stages of the reaction process. This suggests that induction times measured using different experimental techniques are not necessarily equivalent.

I. Introduction

Shock-wave-induced decomposition of energetic materials has long been a subject of considerable interest.[1] In particular, nitromethane (NM) has been heavily studied as a prototypical high explosive.[1−7] Despite these efforts, many details of the shock-induced decomposition of this material are not understood, particularly at the molecular level.[2,8] Previous shock work on neat NM has concentrated on continuum measurements, which have provided information about the kinetics of the shock-induced reaction.[3−7] However, it is not clear what stage of the reaction is controlling the kinetics, since the reaction had already proceeded to a considerable extent by the time it was manifested at the continuum level. In the past, measurements of the induction time for the shock-induced reaction were analyzed by assuming that the kinetics were independent of pressure.[6] However, results from static high-pressure experiments indicate a significant pressure dependence of the reaction rate.[9−12]

Time-resolved optical spectroscopy methods can be used to address these issues. Since the results are sensitive to changes at the molecular level, shock-induced reactions can be observed at the early stages and the kinetics of the early reaction stages can be probed. Also, by varying the initial temperature of the sample, the temperature of the shocked state can be changed without a significant change in pressure.[4] By decoupling pressure and temperature, the effect of pressure on the reaction kinetics can be examined.

Recently, time-resolved absorption spectroscopy was used to examine shock-induced reaction in NM sensitized by ethylenediamine (EDA).[13] These measurements revealed the absorption signature of reaction onset under stepwise loading to 14 GPa peak pressure and the kinetic behavior of the initial stages of the reaction. However, shock-induced decomposition in neat NM was not observed under these conditions.[13]

The objectives of the work described here were (1) to obtain the signature of shock-induced chemical reaction in the absorption spectrum of neat NM and to compare it with the observed spectral changes in sensitized NM, (2) to determine the relative roles of pressure and temperature on the onset of shock-induced reaction in neat NM, and (3) to compare the observed reaction kinetics in absorption experiments with those observed previously in continuum experiments. To meet these objectives, the behavior of the red edge of the nπ* absorption band (peaked at 270 nm) was monitored under stepwise loading. Absorption spectra in the wavelength range 300−550 nm were acquired with a time resolution of 50 ns.

The experimental method is summarized in the next section. Shock-induced changes in the absorption spectrum of neat NM are presented in section III. Section IV presents a discussion of the results, including a comparison with earlier absorption spectroscopy results on NM/EDA mixtures.[13] The reaction kinetics are also analyzed and compared with results from continuum measurements.[6] The main findings are summarized in section V.

II. Experimental Method

All experiments described here were performed using neat nitromethane (NM) as the sample material. This chemical was supplied by Aldrich Chemical Co., Inc., with a nominal purity of 99+%. It was used as received without further purification.

The experimental configuration used in this work was nearly identical with that used in earlier experiments.[13] Therefore, the

[⊗] Abstract published in *Advance ACS Abstracts,* November 1, 1997.

S1089-5639(97)01833-1 CCC: $14.00

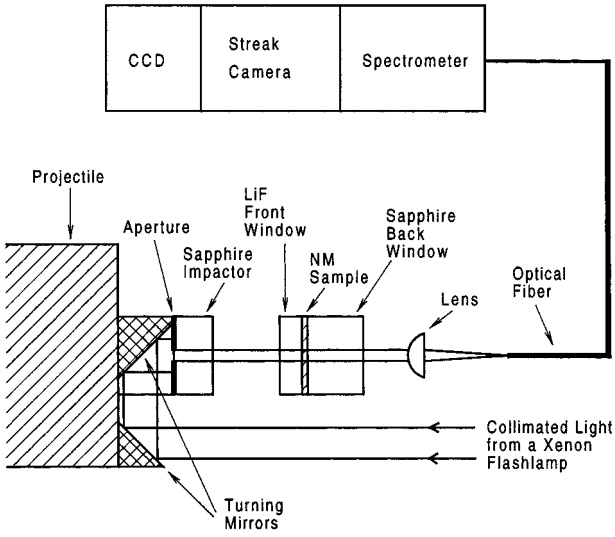

Figure 1. Schematic diagram of experimental configuration.

description of these experiments, except for new features, will be very brief. Details can be seen elsewhere.[14]

A. Overview of the Method. The overall experimental configuration is shown schematically in Figure 1. Light from a xenon flashlamp (10 μs pulse duration) was collimated and directed through the impactor and sample cell using turning mirrors. The transmitted light was collected by a fused silica lens and focused into an optical fiber. This light was spectrally dispersed by a spectrograph and then temporally dispersed by an electronic streak camera. The streak camera output was recorded on a Spex Spectrum One CCD detector (except for experiments 1 and 2, where a vidicon detector was used) as a series of transmission spectra, each separated in time by 50 ns.

The sample cell was similar to that described earlier.[13] A new feature, however, was the ability to heat the cell prior to performing the shock wave experiment. This was accomplished by cutting a groove around the outside of the cell and wrapping a coil of nichrome wire. The cell temperature was monitored by inserting small thermocouples into holes drilled in the brass cell body. The nichrome wire and the thermocouples were potted in place with refractory cement.

The shock waves were generated by projectile impact, where the projectile and the sapphire impactor were accelerated to the desired velocity using a light-gas gun.[15] Upon impact with the front window of the sample cell, a plane shock wave was launched through the front window and into the NM sample. Reverberation of the shock wave between the front and back windows then subjected the liquid sample to stepwise loading (SWL). The peak pressure reached in the SWL process was maintained for approximately 900 ns after the shock entered the sample. The experiment was terminated when release waves from the edge of the impactor converged in the central region of interest.

B. Use of a LiF Front Window. In previous absorption work,[13] sapphire crystals were used for both the front and back windows. This limited the peak pressure attainable in the NM to about 14 GPa, which is near the Hugoniot elastic limit (HEL) of the sapphire crystals.[16,17] Above this stress level, light transmission was lost soon after the shock wave entered the window.[17] To overcome this limitation, ⟨100⟩-oriented lithium fluoride (LiF) crystals[18] were used for the front window (38.1 mm by 3 mm thick disk), while *a*-axis sapphire[19] was used for the impactor (31.7 mm by 15.9 mm thick disk) and the back window (25.4 mm by 12.7 mm thick disk). LiF was previously

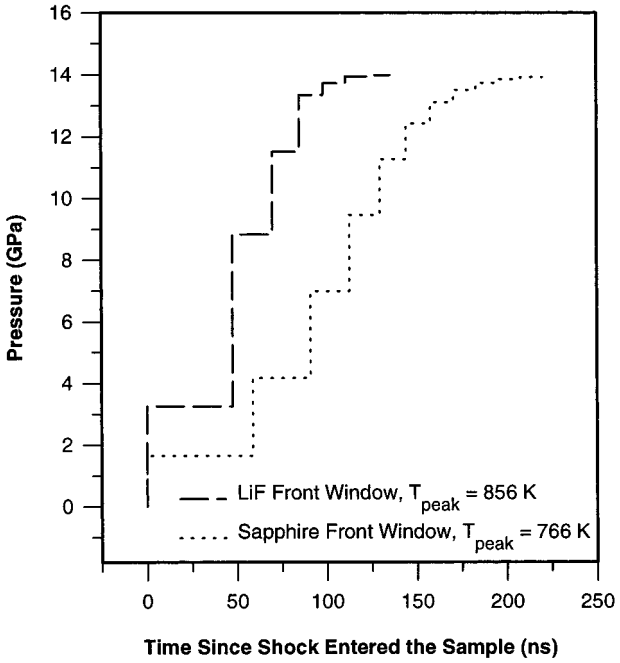

Figure 2. Loading profiles for LiF and sapphire front windows. Peak pressure and temperature in the sample are indicated.

shown to transmit visible light under shock loading to over 100 GPa.[20]

With the LiF front window, peak sample pressures as high as 19 GPa were reached in the present experiments without exceeding an impact stress of 12 GPa in the sapphire impactor. The sapphire back window, on the other hand, had to sustain a stress level equal to that in the NM sample. The experimental results presented here show that, under conditions of stepwise loading due to the shock wave reverberation in the NM sample, the sapphire back window was able to transmit light at stresses as high as 19 GPa.

The presence of the LiF front window also changed the loading history of the NM sample. Figure 2 shows the pressure−time profiles, in the NM samples, for a cell using a LiF front window and for a cell with a sapphire front window. For a given peak pressure, the LiF front window caused a larger first shock in the NM sample and the peak pressure was attained in fewer steps. This resulted in a higher final temperature in the NM sample for a LiF front window compared to a sapphire front window, for a given peak pressure.[14]

C. Thermodynamic Calculations and Methods of Data Analysis. Pressure and temperature profiles for the NM sample were calculated by using either the SHOCKUP[21] or COPS[22] computer codes. Since the peak pressure in the NM sample was related only to the projectile velocity and the shock response of the sapphire and LiF windows, it could be determined very accurately (1−2%). In contrast, temperature calculations depend heavily on the NM equation of state (EOS).

The EOS used in this work was developed in our laboratory.[14,23] It used the Hugoniot for liquids, presented by Woolfolk et al.,[24] with the parameters adjusted to fit the available NM Hugoniot data.[25,26] The specific heat model was based on a single Einstein oscillator with a volume-dependent Einstein temperature. The pressure−temperature coefficient, $(\partial P/\partial T)_v$, was calculated using both the Hugoniot curve[24] and an isotherm derived from the data of Hartmann et al.[27,28]

To determine the absorbance of the NM sample, reference transmission spectra were recorded, prior to the experiment, with the cell filled with hexane. Hexane was used because it has no absorption bands in our wavelength range and its index of

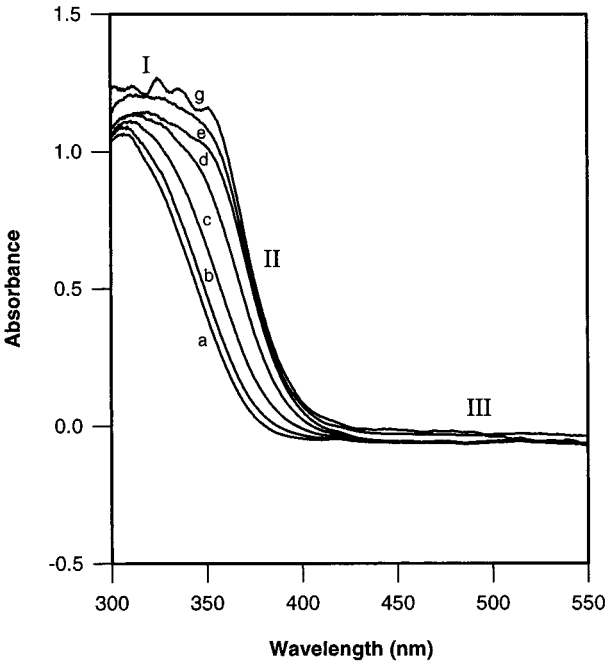

Figure 3. Absorption spectra of NM shocked to 13.8 GPa (experiment 1). Time relative to when the shock reaches the sample: (a) 0 ns, (b) 50 ns, (c) 100 ns, (d) 150 ns, (e) 200 ns, (f) 600 ns, (g) 850 ns.

refraction matches that of NM in the visible region of the spectrum. The cell was then filled with NM and transmission spectra were recorded as the NM was shocked. The absorbance was then calculated as

$$A(\lambda,t) = \log\left(\frac{I_r(\lambda,t) - I_0(\lambda,t)}{I(\lambda,t) - I_0(\lambda,t)}\right) \quad (1)$$

where $A(\lambda,t)$ is the absorbance as a function of wavelength and time, I is the transmitted intensity recorded during the shock, I_r is the intensity transmitted through the hexane reference sample, and I_0 is the background intensity recorded with the streak camera shutter closed.

To determine the position of the absorption band edge, each absorption spectrum was divided into three spectral regions, as shown in Figure 3. The spectral region marked "I" is a region of saturation in the absorption spectra due to instrument effects; the spectral region marked "II" is the region of the absorption band edge; and the spectral region marked "III" is the baseline region where no significant absorption occurs. The absorption band edge region and the baseline region were each fitted with a straight line. The intersection of these two lines was defined as the position of the band edge.

III. Experimental Results

The experimental results are summarized in Table 1. A total of eight absorption experiments with NM samples are presented. Experiments 1−3 used a cell configuration that, apart from the LiF front window, was the same as in ref 13. In experiments 4−7, the sample cell was heated prior to shocking the sample. In experiment 8, the sample cell was modified, as in ref 13, to allow unloading of the sample pressure after peak pressure was reached. The sample thickness, initial temperature, and projectile velocity are measured values, except as noted. The peak pressure and peak temperature were calculated as indicated in the previous section. In all experiments, peak pressures and peak temperatures were achieved within 150 ns of when the shock entered the sample. The band edge shift at peak pressure and the induction time are not listed for experiment 8 because the small sample thickness made it difficult to define the band edge position.

Selected absorption spectra for experiment 1 are shown in Figure 3, where the spectra were smoothed (10 point running average) to reduce the noise due to the vidicon detector. The absorption band edge shows a measurable red-shift as the pressure in the sample rises. After peak pressure is reached, there are no further spectral changes during the experimental time window, which, in this experiment, extends 850 ns after the shock reaches the sample.

At higher pressures and temperatures, additional spectral changes are observed. Unsmoothed absorption spectra from experiment 3 are shown in Figure 4. As in experiment 1, there is a red-shift of the band edge as the sample pressure increases. However, after peak pressure is reached (spectrum d) and the sample pressure becomes constant, additional shifting is observed, followed immediately by a broadband loss of transmission in the sample.[29]

Experiment 5 was performed to determine the effect of a modest increase in the initial sample temperature. As shown in Figure 5, the band edge initially shows little change in position after peak pressure is reached. However, at about 600 ns after the shock wave reaches the sample, the band edge begins renewed red-shifting. Following the start of this additional red-shift, an increase in optical attenuation is observed. The order of events is identical with that of experiment 3 (shown in Figure 4); however, the time scale is significantly different.

In prior work on neat NM,[13] it was shown that the band edge shifting that occurred during the stepwise loading process was reversible under pressure unloading. In the present work, experiment 8 was performed to test the reversibility of spectral changes that occurred after peak pressure was reached. In this experiment, the pressure unloading was accomplished by using a thinner sapphire back window (1.6 mm) so that a rarefaction wave from the free surface of this window arrived in the sample about 350 ns after the shock wave first entered the sample. This rarefaction wave caused a reduction in the sample pressure to approximately 7.0 GPa at 450 ns after the shock wave initially entered the sample. Absorption spectra from experiment 8 are shown in Figure 6. After reaching peak pressure (spectrum c), continued band edge shifting and a loss of optical transmission are observed. This red-shift and the loss of transmission are not reversed when the sample pressure is partially unloaded (spectrum h).[30]

IV. Discussion of Results

A. Shock-Induced Spectral Changes. The spectral changes resulting from stepwise loading of the sample are summarized. The band edge shift profiles, the observed loss of optical transmission through the cell, and the relationship of these results to previous work on sensitized NM are discussed.

1. Interpretation of Absorption Band Edge Shifts. The band edge positions as a function of time, for five representative experiments (experiments 2−6), are shown in Figure 7. In this figure, the peak pressure and peak temperature (from Table 1) are shown for each experiment. The first 150 ns of the profiles in Figure 7 correspond to the period of pressure increase during the reverberation of the shock wave in the sample. During this time period, the band edge shows a shift to longer wavelengths. When peak pressure is reached, the band edge shift reaches a plateau, indicating that the initial shift is a result only of the compression from the stepwise loading. As shown in Figure 7, experiments having a peak temperature above 940 K exhibit renewed band edge shifting within the time duration of our experiments. Since no changes in the pressure and temperature

TABLE 1: Summary of Experimental Results

expt. no.	sample thickness (μm)	initial temp (K)	projectile velocity (km/s)	calc peak pressure (GPa)	calc peak temp (K)	calc time to reach peak pressure (ns)	band edge shift (nm)	induction time (ns)
1	164	298[a]	0.766	13.8	854	149	22.5	>850
2	139	298[a]	0.936	17.3	946	111	29	800
3	174	298[a]	1.024	19.1	996	131	36.5	200
4	162	324	0.768	13.9	899	147	28	>800
5	156	348	0.793	14.4	957	138	30.5	600
6	155	319	0.929	17.1	985	124	30.5	300
7	154	320	0.933	17.2	988	123	41.5	250
8[b]	96	324	0.921	17.0	985	77	*c*	*c*

[a] Nominal value. [b] Unloading experiment. [c] Not applicable.

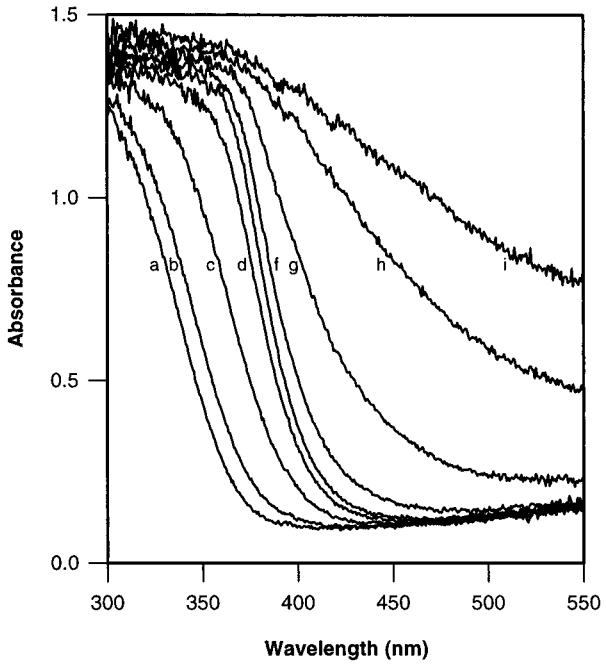

Figure 4. Absorption spectra of NM shocked to 19.1 GPa (experiment 3). Time relative to when the shock reaches the sample: (a) 0 ns, (b−d) 50−150 ns, (e−i) 200−400 ns. The time interval between spectra is 50 ns. Peak pressure is attained at 131 ns.

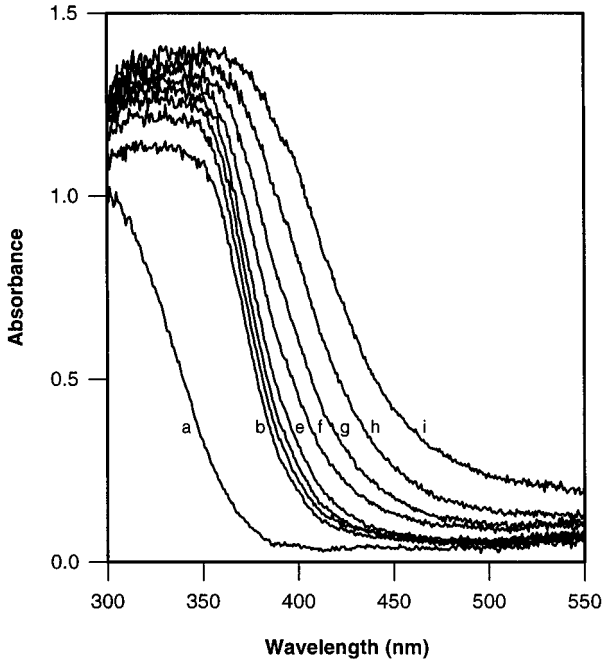

Figure 5. Absorption spectra of NM shocked to 14.4 GPa (experiment 5). Initial temperature = 348 K. Time relative to when the shock reaches the sample: (a) 0 ns, (b) 200 ns, (c) 450 ns, (d−i) 550−800 ns (50 ns intervals). Peak pressure is attained at 138 ns.

of the sample are introduced after peak pressure is reached, the renewed shifting is indicative of the onset of a chemical reaction. Figure 7 also shows that the timing of the reaction onset is related to the peak temperature in the sample. This is discussed later in more detail.

Figure 7 shows that the shift of the absorption band edge is comprised of two components: a compression-induced shift and a reaction-induced shift. The compression-induced shift in neat NM has been observed previously.[13] It was shown to be reversible under pressure unloading, indicating that no irreversible chemical changes were occurring.

The reaction-induced shift in neat NM, reported here for the first time, appears later in time after peak pressure is reached (Figure 7). The results of experiment 8, an unloading experiment shown in Figure 6, establish the irreversibility of these spectral changes under the reduction of pressure and temperature.

The origin of the reaction-induced shift cannot be conclusively identified from these absorption data. However, it is likely that, with reaction-induced changes in the electronic structure of the molecules, the nπ* transition is enhanced and broadened. This is reasonable since the nπ* transition is forbidden in the local C_{2v} symmetry of the NO_2 group.[31,32] As the reaction occurs, this symmetry restriction is likely to be lifted, causing the observed changes in the band edge.

2. Interpretation of the Loss of Transmission through the Sample Cell. When the reaction-induced band edge shift was observed, it was quickly followed by the loss of light transmission through the sample cell. Window failure was ruled out as the cause of this transmission loss through the use of hexane experiments.[29,30] Therefore, this loss of light transmission is ascribed to chemical reaction.

The reaction-induced loss of transmission must be due to the formation of reaction products that attenuate visible light. This limits the number of possible explanations, since most small organic molecules and radicals absorb only in the UV.[33] One candidate molecule is nitrogen dioxide, which is known to absorb over much of the visible spectrum[33] and, with the expected pressure broadening of the absorption bands,[34] could account for the observed attenuation. However, opacity in shocked NM has also been attributed to the formation of small particles of free carbon.[35] Hence, a definitive conclusion cannot be drawn from the present work.

3. Comparison with Work on NM/EDA Mixtures. The behavior of the absorption spectrum of neat NM under shock loading is substantially different from that of amine-sensitized NM. The differences between neat and sensitized NM have already been observed and analyzed for stepwise loading up to approximately 14 GPa peak pressure.[13]

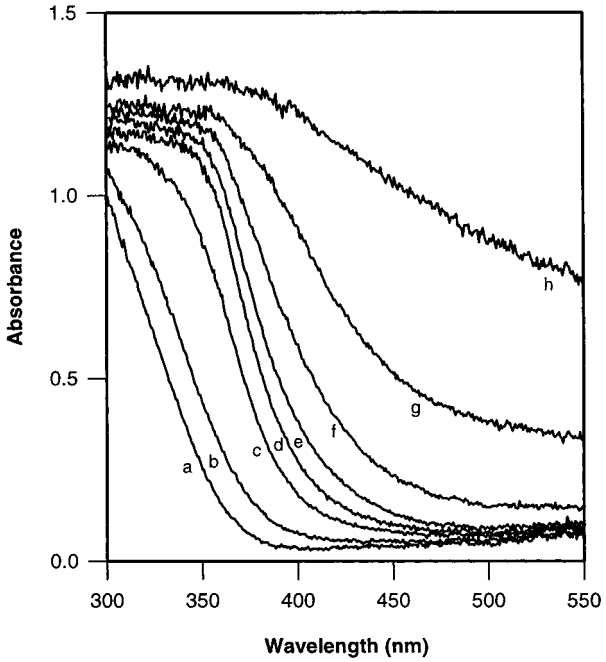

Figure 6. Absorption spectra of NM shocked to 17.0 GPa (experiment 8). Initial temperature = 324 K. Time relative to when the shock reaches the sample: (a−g) 0−300 ns (50 ns intervals), (h) 450 ns. Spectra c−g were taken at peak pressure. spectrum h was taken after unloading to about 7.0 GPa.

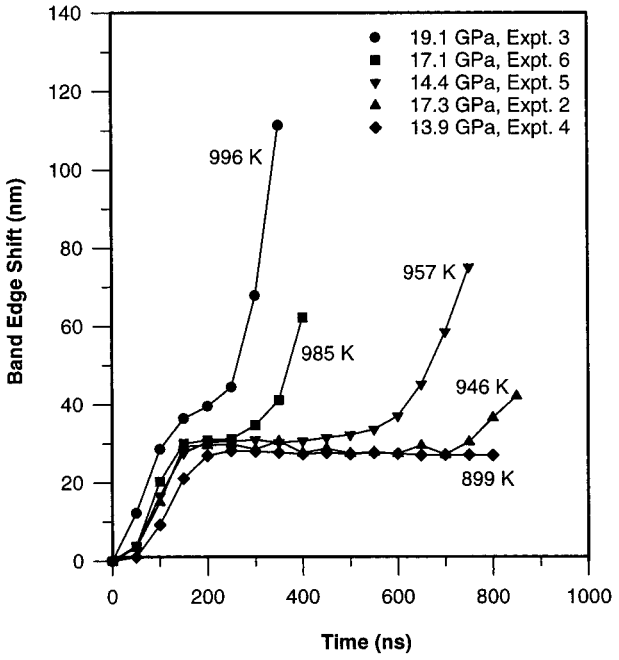

Figure 7. Absorption band edge shifts of shocked NM. Time is relative to when the shock reaches the sample. Peak shock temperatures, from Table 1, are displayed with the curves.

The time profile of the reaction-induced band edge shift in neat NM from the present work can be compared with earlier band edge shift profiles from a NM/EDA mixture and from neat NM. Figure 8 shows a plot of the band edge shift versus time for experiment 5, which reached a peak pressure of 14.4 GPa (957 K), and for previous experiments[13] on neat NM and a NM/EDA mixture, which reached peak pressures of 14.5 GPa (775 K) and 13.2 GPa (755 K), respectively. Due to a faster rise in pressure, the shock-induced shift in the band edge occurs more quickly in experiment 5 than in the previous experiments. The magnitude of the shock-induced shift at peak pressure is also

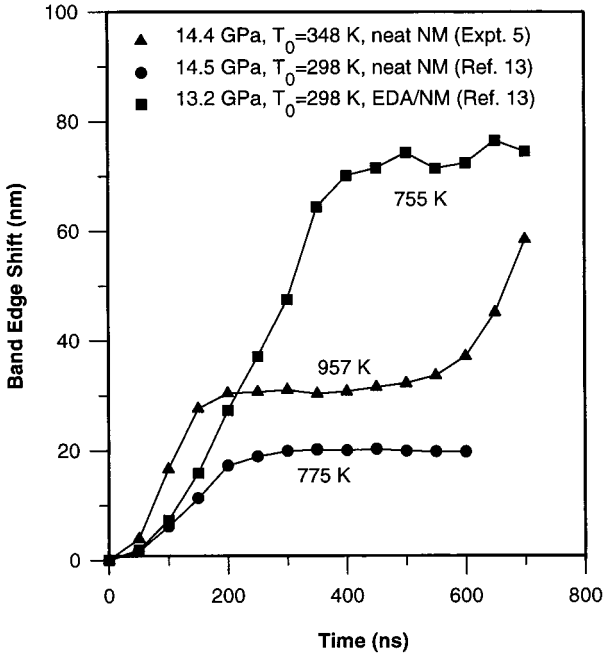

Figure 8. Comparison of absorption band edge shifts of neat NM and sensitized NM (0.1% EDA in NM) under stepwise loading. Time is relative to when the shock reaches the sample. Peak pressures, peak temperatures, and initial temperatures are displayed along with the data.

greater in experiment 5 than in the experiment on neat NM from ref 13. This is presumably due to the higher peak temperature in experiment 5.

The most interesting feature of Figure 8 is the marked difference in the onset of the reaction-induced band edge shift for neat NM relative to sensitized NM. Unlike neat NM, sensitized NM does not show any time delay before exhibiting reaction-induced spectral changes. Also, the leveling-off of the reaction-induced band edge shift, which is observed in sensitized NM, is not observed in neat NM. On the contrary, the lack of band edge data beyond 700 ns in experiment 5, shown in Figure 8, is due only to a loss of optical transmission through the sample, and not a termination of the band edge shift. The plateau in the band edge shift of sensitized NM and the previously observed partial reversibility of this shift have been attributed[13] to quenching of the reaction after initiation at localized sites around the amine molecules. However in neat NM, on the basis of the time profiles of band edge shifts and the irreversibility of these shifts, it appears that the reaction initiates and then grows rapidly without quenching.

Unlike the response of neat NM at higher pressures (Figure 4), no broadband loss of transmission was observed in sensitized NM before the end of the experiment at 14 GPa peak pressure.[13] This suggests a difference in the reaction products that are produced in the early stages of the reaction.

The differences in the reaction-induced shifts and the broadband transmission loss between neat NM and the NM/EDA mixture indicate that the addition of EDA to NM causes changes in the kinetics of the early stages of shock-induced decomposition. These changes result from one of two sources: The difference in the kinetic behavior for the EDA-sensitized NM relative to neat NM may result from a change in the mechanism of decomposition. Alternatively, the difference in behavior may result from an alteration of the initial reaction conditions, producing kinetic changes without changing the overall reaction mechanism. However, it is not possible to rule out either alternative based solely on the data presented here. More work is needed to fully address this issue.

B. Analysis of Induction Times. The induction time (defined as the length of time from when the shock wave enters the sample to the onset of reaction) provides a measure of the kinetics of the reaction because it can be related, through kinetic models, to the reaction rate.[36] In practice, the length of the induction time depends on the experimental probe that is used to detect the onset of reaction. In the absorption experiments reported here, the end of the induction time is defined by the appearance of the reaction-induced band edge shift.

1. Thermal Explosion Theory and Comparison with Continuum Work. The induction time of NM has been the subject of previous shock initiation studies.[3−6] These studies focused on the macroscopic (i.e. continuum) properties of the material. The work of Hardesty[6] was a particularly detailed study. He used the VISAR technique,[37] under single shock loading conditions, to measure the particle velocity in the sample. He also recorded streak camera photographs of the light emitted from the sample. The onset of reaction (the end of the induction time) was indicated by a sudden rise in the sample pressure and by the sudden emission of light from the sample. We expected that the induction times reported previously[6] would be longer than those measured in the absorption experiments reported here because the continuum measurements probed events which were believed to occur after a larger fraction of the sample was consumed by the reaction.

Hardesty interpreted his data according to the thermal explosion model of shock initiation.[6,36,38] This model assumes that the induction time is controlled by an exothermic reaction where the reaction rate is determined primarily by the sample temperature.[36] In a combustion process, this assumption implies that the reaction proceeds minimally during the induction period.[36] The reaction rate is assumed to have an Arrhenius dependence on temperature,

$$\frac{dC_{NM}}{dt} = f(C_{NM}) \exp\left(\frac{-E_A}{RT}\right) \tag{2}$$

where C_{NM} is the concentration of unreacted NM, E_A is the activation energy, and $f(C_{NM})$ is the concentration-dependent kinetic function that describes the assumed rate law. Because the reaction is assumed to proceed minimally during the induction time, the kinetic function changes little during this time. The thermal explosion model is therefore not sensitive to the specific rate law used.[39] As a first approximation, the kinetic function can be assumed constant,[36]

$$f(C_{NM}) \approx A \tag{3}$$

where A is a constant. According to the thermal explosion model, the induction time is then given by[36]

$$\tau = \left(\frac{c_v}{QA}\right)\left(\frac{RT^2}{E_A}\right) \exp\left(\frac{E_A}{RT}\right) \tag{4}$$

where c_v is the specific heat at constant volume and the heat of reaction is designated by Q.

For the purpose of comparison with previous continuum results, the thermal explosion model can be applied to our absorption data. The induction times taken from the VISAR data of Hardesty[6,38] and from the absorption data reported here (see Table 1) are plotted against temperature in Figure 9. These induction time data were fitted with the following function:

$$\tau = \left(\frac{c_v}{QA}\right)\left(\frac{RT^2}{E_A}\right) \exp\left(\frac{E_A}{RT}\right) = \left(\frac{a_0}{a_1}\right) T^2 \exp\left(\frac{a_1}{T}\right) \tag{5}$$

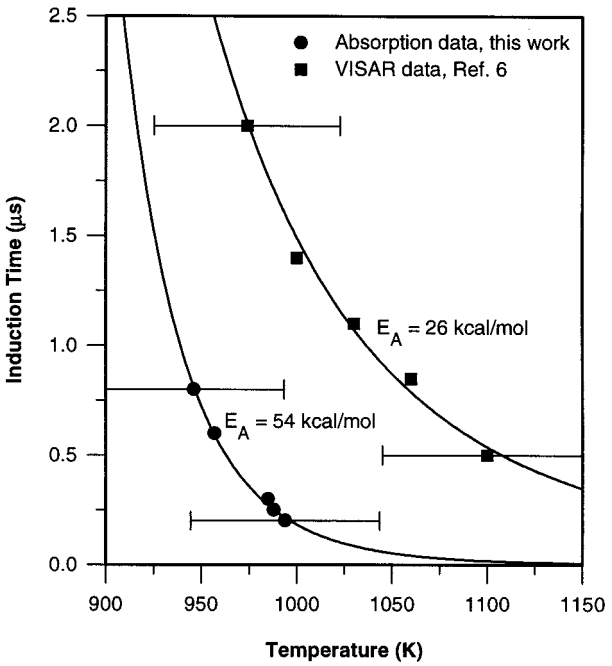

Figure 9. Comparison of induction time data. The curves are fits to the data using eq 5. The estimated activation energies shown are derived from the fits.

where $a_0 = c_v/QA$ and $a_1 = E_A/R$. Fits of eq 5 to the data, using a_0 and a_1 as fitting parameters, are included in Figure 9. The temperatures for both sets of data were calculated using our equation of state.[14,23] The error bars were calculated by assuming a 5% uncertainty in the temperature values. Figure 9 shows that both sets of data are fitted quite well with the function in eq 5, providing support for the thermal explosion model. The estimated activation energies obtained from the fits in Figure 9 are 54 kcal/mol for the absorption data and 26 kcal/mol for the VISAR data. These activation energies have large uncertainties due to the uncertainty in the temperature calculations. Hence, they are presented for the purpose of comparison only. The absolute value of these activation energies should not be taken too seriously without more precise temperature calculations.

Despite the difference between the stepwise loading conditions of our absorption experiments and the single-shock conditions of the VISAR experiments,[6] the large difference in the activation energy of the two data sets does not necessarily indicate that the reaction mechanisms are different in the two cases. The absorption measurements and the VISAR measurements[6] probe different stages of the reaction process. The VISAR measurements are sensitive to changes in pressure and density that occur after the reaction has proceeded to a considerable extent. In contrast, the absorption results are sensitive to changes at the molecular level. These changes can be detectable, in low concentration, early in the reaction process, before appreciable changes in pressure and density occur. This difference in sensitivity led to longer induction times, for a given temperature, for the VISAR work relative to the absorption work. Caution must therefore be used when comparing induction time data obtained using different experimental techniques. To obtain a more reliable comparison of the decomposition kinetics under single-shock and stepwise loading conditions, experiments need to be performed where the same measurement technique is used under both loading conditions. It would therefore be of interest to perform VISAR measurements under stepwise loading conditions similar to those in our absorption experiments.

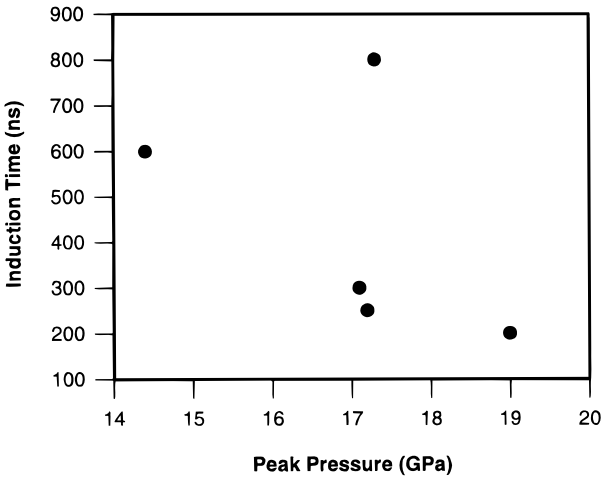

Figure 10. Correlation of induction time with peak pressure.

2. Role of Temperature versus Pressure. Despite the difficulties in obtaining accurate activation energies from the induction time data, qualitative information regarding the reaction can be extracted. For instance, these data can be used to explain the observed reduction in the induction time caused by raising the initial temperature of the sample. This effect was observed previously[3,4] under single-shock loading conditions, but a careful analysis of the phenomenon was not performed.

From Figure 9, it is clear that the reaction kinetics after stepwise loading correlate well with the peak temperature. Calculations performed using our equation of state have shown that an increase in the initial sample temperature causes a resultant (but larger) increase in the peak sample temperature after stepwise loading. The observed decrease in the induction time is therefore a simple temperature effect and is not due to fundamental changes in the initial properties of the material.

The induction time data also yield information on the pressure dependence of the reaction rate. Figure 10 shows that the correlation of the induction time with peak pressure for the absorption experiments is quite poor. For the three experiments with 17 GPa peak pressure, the large spread in induction time values indicates the relative weakness of any pressure effects. In contrast, the correlation of the induction time with peak temperature was shown to be very good in Figure 9. Additional evidence for the weakness of any pressure effects comes from the ability of the thermal explosion model to fit data for pressures ranging from 14 to 19 GPa, even though the underlying theory contains no dependence on the sample pressure. The success of the thermal explosion model suggests a negligible pressure dependence for the reaction mechanism over the range of pressures examined here.

The lack of a significant pressure effect in the reaction kinetics is in contrast to thermal decomposition work under static high pressure, where the reaction rate was found to have a substantial pressure dependence.[9−12] However, the static high-pressure work was performed on NM in the solid phase, whereas NM is believed to remain as a metastable liquid under shock conditions.[13] It is possible that different phases of NM will have different decomposition mechanisms. In addition, NM becomes quite stiff at high pressure. Our equation of state calculations indicate that the difference in density compression between stepwise loading to 14 and 19 GPa is only about 5%. Therefore, in the pressure range examined here, pressure effects that do exist are expected to be too small to be observed.

V. Conclusions

Shock-induced changes, indicative of chemical reaction, have been observed in the UV−visible absorption spectrum of neat NM subjected to stepwise loading. Extensive reaction was indicated by irreversible red-shifting of the band edge which occurred after peak pressure was reached in the sample. This reaction-induced red-shift was followed by a loss of transmission through the sample, which was attributed to the formation of absorbing reaction products. Comparison of the reaction-induced spectral changes in neat NM with those in EDA-sensitized NM[13] suggests that the presence of the amine causes a change in the early stages of shock-induced decomposition.

An induction time was observed between the beginning of stepwise loading and the onset of reaction-induced spectral changes. Large decreases in the induction time were produced by modest increases of 25 to 50 K in the initial sample temperature, due to the resultant increase in the final shock temperature. The induction time data are consistent with the thermal explosion model of shock initiation in energetic materials. The observed induction time correlates only with the final shock temperature, as assumed by the theory. The induction time data exhibit no observable pressure dependence within the pressure range examined here. Measured induction times for the absorption experiments are consistently shorter than for VISAR experiments[6] reaching similar temperatures likely because the absorption measurements probe earlier stages of the reaction process. This suggests that induction times measured using different experimental techniques are not necessarily equivalent, which helps to explain the large differences in the estimated activation energies.

Acknowledgment. Useful discussions with Dr. C. P. Constantinou and Dr. G. I. Pangilinan are gratefully acknowledged. D. Savage and K. Zimmerman are both thanked for their expert assistance in the experimental effort. Prof. G. E. Duvall is sincerely acknowledged for his important role in the development of the NM equation of state used in this work. Dr. T. Allen is thanked for performing the hexane experiment discussed in ref 30. This work was supported by ONR Grants N00014-90-J-1400 and N00014-93-1-0369. The enthusiastic interest of Dr. R. S. Miller is sincerely appreciated.

References and Notes

(1) See proceedings of the *First through Tenth Symposia (International) on Detonation*; Office of Naval Research: Arlington, Virginia, 1951−1993.

(2) Cheret, R. *Detonation of Condensed Explosives*; Springer-Verlag: New York, 1993.

(3) Campbell, A. W.; Davis, W. C.; Travis, J. R. *Phys. Fluids* **1961**, *4*, 498.

(4) Voskoboinikov, I. M.; Bogomolov, V. M.; Apin, A. Ya. *Fizika Gor. Vzryva* **1968**, *4*, 45.

(5) Berke, J. G.; Shaw, R.; Tegg, D.; Seely, L. B. In *Fifth Symposium (International) on Detonation*; Office of Naval Research: Arlington, Virginia, 1970; p 237.

(6) Hardesty, D. R. *Combust. Flame* **1976**, *27*, 229.

(7) Walker, F. E.; Wasley, R. J. *Combust. Flame* **1970**, *15*, 233.

(8) Gupta, Y. M. *J. Phys. IV, Colloq. C4* **1995**, *5*, C4−345.

(9) Lee, E. L.; Sanborn, R. H.; Stromberg, H. D. In *Fifth Symposium (International) on Detonation*; Office of Naval Research: Arlington, Virginia, 1970; p 331.

(10) Shaw, R.; DeCarli, P. S.; Ross, D. S.; Lee, E. L.; Stromberg, H. D. *Combust. Flame* **1979**, *35*, 237.

(11) Piermarini, G. J.; Block, S.; Miller, P. J. *J. Phys. Chem.* **1989**, *93*, 457.

(12) Rice, S. F.; Foltz, M. F. *Combust. Flame* **1991**, *87*, 109.

(13) Constantinou, C. P.; Winey, J. M.; Gupta, Y. M. *J. Phys. Chem.* **1994**, *98*, 7767.

(14) Winey, J. M. Time-Resolved Optical Spectroscopy to Examine Shock-Induced Decomposition in Liquid Nitromethane. Ph.D. Dissertation, Washington State University, 1995.

(15) Fowles, G. R.; Duvall, G. E.; Asay, J.; Bellamy, P.; Feistmann, F.; Grady, D.; Michaels, T.; Mitchell, R. *Rev. Sci. Instrum.* **1970**, *41*, 984.

(16) Barker, L. M.; Hollenbach, R. E. *J. Appl. Phys.* **1970**, *41*, 4208.

(17) Webb, R. L. Transmission of 300−500 nm Light Through Z-cut Sapphire Shocked Beyond Its Elastic Limit. M.S. Thesis, Washington State University, 1990.

(18) Bicron Corp., Solon, OH.

(19) Union Carbide, Inc., Washougal, WA.

(20) Wise, J. L.; Chhabildas, L. C. In *Shock Waves in Condensed Matter−1985*; Gupta, Y. M., Ed.; Plenum Press: New York, 1986; p 441.

(21) SHOCKUP code; Ogilvie, K. M.; Duvall, G. E.; Collins, R. (Washington State University, Pullman, WA, 1984) unpublished.

(22) COPS code; Gupta, Y. M. (Stanford Research Institute, Menlo Park, CA, 1978) unpublished.

(23) Winey, J. M.; Knudson, M. D.; Duvall, G. E.; Gupta, Y. M. *Bull. Am. Phys. Soc.* **1997**, *42*, 1507.

(24) Woolfolk, R. W.; Cowperthwaite, M.; Shaw, R. *Thermochim. Acta* **1973**, *5*, 409.

(25) Lysne, P. C.; Hardesty, D. R. *J. Chem. Phys*. **1973**, *59*, 6512.

(26) Marsh, S. P., Ed. *LASL Shock Hugoniot Data*; University of California Press: Los Angeles, 1980.

(27) Hartmann, H.; Neumann, A.; Schmidt, A. P. *Ber. Bunsen-Ges. Phys. Chem.* **1968**, *72*, 877.

(28) Isaacs, N. S. *Liquid-Phase High-Pressure Chemistry*; John Wiley and Sons: New York, 1981; p 100.

(29) To verify that the attenuation observed in experiment 3 was indeed due to changes in the NM sample, rather than the windows, an absorption experiment was performed with a hexane sample. The sample cell was observed to retain transparency for about 600 ns after the shock entered the sample. This is 200 ns longer than was observed with a NM sample in experiment 3, showing that the early onset of opacity in experiment 3 was due to changes in the NM sample, and not failure of the cell windows.

(30) A hexane experiment was performed, in the unloading configuration, to verify that the irreversible loss of transmission was not due to a failure of the sapphire back window. This experiment, which reached a peak pressure of 16.8 GPa before unloading to about 7.0 GPa, showed that the hexane cell retained transparency for at least 700 ns after the shock reached the sample.

(31) Bayliss, N. S.; MacRae, E. G. *J. Phys. Chem.* **1954**, *58*, 1006.

(32) Flicker, W. M.; Mosher, O. A.; Kuppermann, A. *Chem. Phys. Lett.* **1979**, *60*, 518.

(33) Herzberg, G. *Molecular Spectra and Molecular Structure, III. Electronic Spectra and Electronic Structure of Polyatomic Molecules*; Van Nostrand Reinhold Co.: New York, 1966.

(34) Drickamer, H. G.; Frank, C. W. *Electronic Transitions and the High-Pressure Chemistry and Physics of Solids*; Chapman and Hall: London, 1973.

(35) Yakusheva, O. B.; Yakushev, V. V.; Dremin, A. N. *High Temp.-High Press.* **1971**, *3*, 261.

(36) Frank-Kamenetskii, D. A. *Diffusion and Heat Exchange in Chemical Kinetics*; Plenum Press: New York, 1969; p 353.

(37) Barker, L. M.; Hollenbach, R. E. *J. Appl. Phys.* **1972**, *43*, 4669.

(38) Hardesty, D. R.; Lysne, P. C. Sandia Laboratories Research Report #SLA-74-0165, 1974.

(39) The insensitivity of the thermal explosion model to changes in the rate law was demonstrated by repeating the fits to the induction time data using a fitting function derived from a second-order rate law. In this analysis, the extent of reaction was taken into account by allowing the kinetic function to vary with the reactant concentration. These fits yielded activation energies that were almost identical with those calculated from eq 5. In a similar way, fits using autocatalytic rate laws resulted in values for the activation energy that deviated only slightly from the values given above.